

# **Agriculture phenology monitoring using NDVI time series based on remote sensing satellites: A case study of Guangdong, China**

Komal Choudhary\*<sup>1,2,4</sup>, Wenzhong Shi<sup>1</sup>, Mukesh Singh Boori<sup>2,3</sup>, Samuel Corgne<sup>4</sup>

<sup>1</sup>The Hong Kong Polytechnic University, Hong Kong, China

<sup>2</sup>Samara National Research University, Samara, Russia

<sup>3</sup>American Sentinel University, Colorado, USA

<sup>4</sup>University of Rennes 2, Rennes, France

## **Abstract**

This article presents the use of the Normalized Difference Vegetation Index (NDVI) time series based change detection method for agriculture phenology monitoring. NDVI makes use of the multi-spectral remote sensing data band combinations techniques to find out landscape such as agriculture, vegetation, land use/cover, water bodies and forest. Geographic Information System (GIS) technology is becoming an essential tool to combine multiple maps and information from different sources such as satellite, field and socio-economic data. Landsat 8 and Sentinel-2 satellite data were used to generate NDVI time series from Sep. 2017 to Nov. 2018. This research work was the procedure by pre-processing, signal filtering and interpolation of monthly NDVI time series that represent a complete crop phenological cycle. NDVI method is applied according to its specialty range from -1 to +1. We divided the whole agriculture area into five parts according to NDVI Values such as no agriculture, low agriculture, medium agriculture, high agriculture and very high agriculture area. The simulation results show that the NDVI is highly useful in detecting the surface feature of the area, which is extremely beneficial for sustainable development of agriculture, and decision making. The methodology of reform NDVI time series has been feasible to improve crop phenology mapping.

**Keywords:** NDVI, GIS, phenology cycle, Landsat, Sentinel

## **1. Introduction**

Remote sensing imagery is extremely significant to acquire a greater knowledge of Earth's ecology. It is the science and art of acquiring information in the form of spectral, spatial, and temporal forms about certain objects, areas such as agriculture, vegetation, LULC classification

and water resources (Ahmadi et al., 2012). Agriculture is a production system that promotes variable management practices within an area according to specific site conditions. This system is based on the new tools and sources of information provided by modern technologies. These include remote sensing techniques, global positioning systems (GPS), geographic information systems (GIS) and different applications (vulnerability, risk assessment, climate change, vegetation etc....). Remote sensing data can be used to accurately estimate crop condition by relationship between multispectral reflectance, crop temperature, photosynthesis etc. which pioneered the technique of combining spectral data and meteorological data for crop growth and yield estimation (Alex et al., 2018). The beneficial use of spatial imagery in agriculture for crop management is known as 1929 when aerial photography was used for mapping of soil. Four major requirements are required for agriculture monitoring: continuous coverage, rapid data distribution, high resolutions, and integration (Atzberger et al., 2013). Remote sensing imagery-based crop management systems help to identify crop area management, soil mapping, crop yield forecasting, seasonal variations, DEM, damage control etc.

Agriculture remote sensing information advantage is the basis of remote sensing application. In depth understanding of the crop rotation process plays an important role in the quantitative remote sensing crop monitoring (Aadhar et al., 2017). Agriculture quantitative remote sensing is an important way to achieve major crop information through NDVI. This field can provide valuable reference information for agriculture management and be used as input data for crop development models. There are several vegetation indices to highlight vegetation areas on the remote sensing scene. NDVI is one of the important topics of crop quantitative remote sensing (Chen et al., 2011, Esch et al., 2014). This is an important agriculture index, which is applied in research on global and local environments. This article shows how the differences between the visible red and near infrared bands of satellite images could be used to identify areas containing important agriculture and vegetation different characteristics.

In the research Sentinel-2 data generalized Normalized Difference Vegetation Index (NDVI) time series with NDVI data derived from Landsat 8 for land-cover mapping. Sentinel-2 data was launched in 2015 (Estel et al., 2016). Landsat- 8 data also has a high resolution which makes it more suitable for mapping crop fields with smaller areas such as the Guangdong provision. This

study has confirmed that phenological features, including the maximum, minimum and NDVI mean values calculated from fused NDVI data, are relevant for classifying various vegetation and agriculture categories such as forest, scrubland, and crop classes. Cropland mapping based on time series analysis is challenged such as (1) the lack of samples used to supervised classification (2) missing temporal data caused by clouds shadowing (3) monthly changes of phenological cycles caused by weather in the agriculture field. Some algorithms, data Fusion and filtering are provided to be a scientific solution to handle these challenges. Remote sensing data used in numerous fields such as: Land use/land cover classification, crop monitoring, soil moisture assessment, soil type categorization, vegetation classification, crop classification, etc. (Fan et al., 2012). In this article, the multispectral image of Guangdong is used to calculate features, such as vegetation, water body, bare land, mangrove, agriculture, settlements, and forest are presented in this image and to subsequently make these extracted features available for further analysis to avoid any kind of natural disasters.

The main aim of this study was the design of a monthly reproducible crop mapping and monitoring, which could face temporarily and spatially fragmented remote sensing data. In addition to the idea of crop phenology, the coordination of spatial precise data on agriculture land use/cover from data sources was an important factor in obtaining desired information (Gnyp et al., 2014). We have collected it for integrating remote sensing and GIS methods based on supporting information and expert knowledge on crop phenology in a multi-data approach. This method has been applied for the monthly crop monitoring from Sep.2017 to Nov.2018. The recognition of the monthly crop mapping system and the results received clearly depicts the high NDVI show in April and September months. The southern part of Guangdong provision in southern China was selected as a study area because crops have been planted there for more than forty years (Gommes et al., 2017) and it is one of the key bases of crop monitoring. Rice is a major crop, which is cultivated twice per year and three crops near the Pearl River delta (Hansen et al., 2012).

The main objectives of this study were: (1) The satellite data and preprocessing expected to allow their meaningful comparison were described (2) Appropriate critical processing methodology including smoothing and monthly NDVI time-series interpolation (3) Remove the phenology

parameters from the NDVI time series to mark the crop rotation events (4) Evaluated the effectiveness of analyzing Sentinel-2 and Landsat-8 data derived phenology parameters.

## 2. Study area

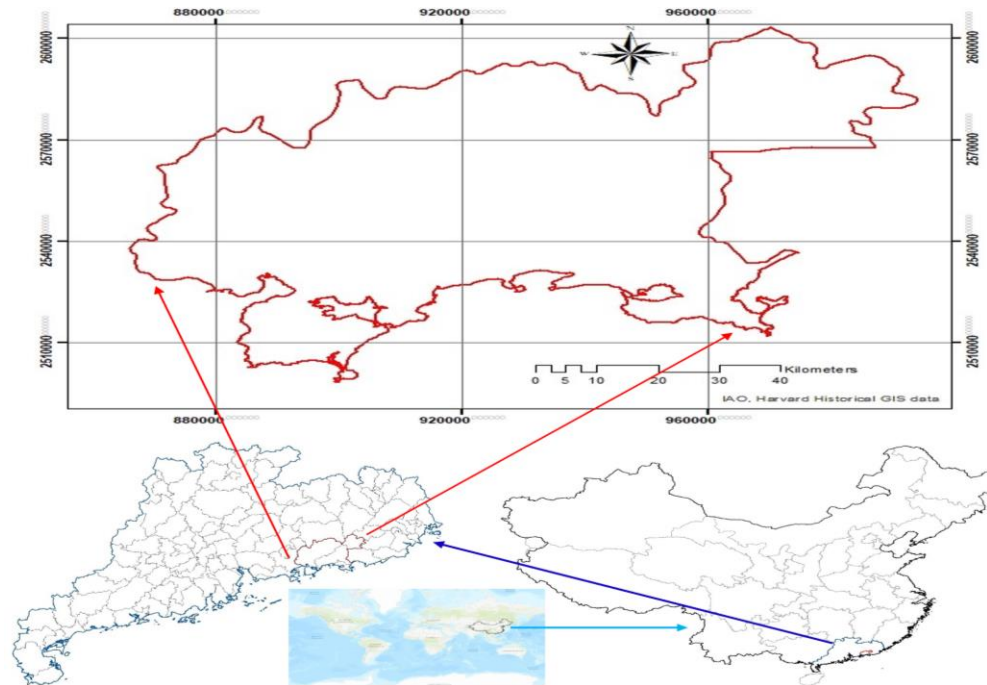


Fig: 1 Location map of the study area in Guangdong, China

Four subdivision parts Huidong (Huizhou), Haifeng (Shanwei), Luhe (Shanwei) and Shanwei (Shanwei) of Guangdong province, China was chosen as a study area (fig. 1). It is in the South China Sea coast with complex geomorphology. Most of the area has a humid subtropical climate. It has a wet season from April to September with long hot and dry seasons. From November to January, it has short and mild weather. February, March, and October are transition months. During these months, the state of wetness can be reduced to a great extent throughout the province. For example, the northern region is often wet, but the south is dry in March and April months. In September, the pattern is reversed. Average daily temperatures in January and July are 18°C (64°F) and 33°C (91°F), respectively, although the humidity makes it feel much hotter in summer.

Rice is the leading crop and other secondary crops are sweet potatoes, peanuts (groundnuts), wheat and tea. Two crops of rice a year can be grown on most cultivated land and near the Pearl River

Delta three crops are not unusual. Several industrial crops, including rubber, sisal, palm oil, coffee, black paper are successfully raised. Also 300 kinds of fruits are grown such as citrus, litchi, pineapple, bananas etc. In general, the province's soils are poor, as high temperatures and plentiful rainfall result in bleaching and leaching. With greater reliance on the use of chemical fertilizers, farming and irrigation have become increasingly mechanized in the study area.

### **3. Materials and methods**

#### ***3.1 Datasets***

To obtain adequate spatial and temporal coverage of the study area monthly and at a lower cost, multispectral data was downloaded from the United States geological survey (USGS) website. We applied Landsat 8 (OLI) and Sentinel-2B data for surface reflectance information. The most modern satellites are Sentinel-2 and Landsat 8, which provide free data for long periods with high-frequency (Harmon et al., 2005). The high-quality satellite images were present in 15 m and 30 m with a 16-day revisit period in Landsat data (He et al., 2017). The latter is equipped with Sentinel-2B multispectral instruments, which can obtain 13 bands information in various spatial proposals such as 10 meters, 20 meters and 60 meters. Sentinel-2 is more advanced than Landsat 8 along with its excellent qualities, such as the rising number of bands, fast repeat time, etc. Sentinel-2B provides more details in the NIR band range and Red bands, which is helpful for agriculture, forest, and vegetation phenological analysis.

#### ***3.2 Pre-processing***

This research work was benefited from ground-based information collected from remote sensing and GIS. We have downloaded all month's images of 2017-2018. Then completed image pre-processing steps like remove all radiometric, geometrics distortion and project all datasets in world geodetic system (WGS-1984 UTM – Zone 50N) projection. After that, all noise or sensors related errors such as droplines was removed and each pixel was geocoded as its exact location on globe and used best band combination to identify specific features in false color composite images (Liang et al., 2015). So finally, all data were vectorized and interpolated as grid datasets so that easy to use in GIS format analysis, which was helping to derive meteorological information, agriculture information and forest information. We also use filters to remove noise in images, enhancement techniques for better feature identification and in last best band combination as NDVI.

### ***3.3 Normalized difference vegetation index (NDVI) time series***

The temporal phenology of the target classes was calculated using the red and near-infrared bands generated NDVI:

$$NDVI = \frac{NIR - Red}{NIR + Red}$$

NDVI is among the most frequently applied vegetation indices in agriculture research (Meng et al., 2009). It was computed using from Red and near-infrared bands in ArcGIS software. The red band was selected as band 4 and the NIR band 8a in the Sentinel-2B satellite to acquire the best possible results for NDVI analysis. We selected NIR band 8a because its wavelength (0.865) is like Landsat 8 NIR band 5 wavelength (0.865) (Sakamoto et al., 2005, Shi et al., 2014). Band 4 is a red band in Landsat 8 OLI. Optical sensors cannot observe earth surface continuously due to cloud cover especially in rainy sessions. Consequently, remote sensing techniques are disrupted by noise resulting from deteriorating atmospheric changes. Thus, noise reduction is necessary before further analysis.

Many regional filtering techniques necessitate the depiction of a time series that constantly and properly interval. Though, there is a difficulty during data collection on some days, due to missing data in a particular time and harsh climatic conditions. However, approached were contacted to manipulate time-series data, the signal processing-based method cannot work well in the location time series data from the same time-period. So, when the time series was used, then a major problem was reconstructing the completeness of time-series dataset.

### ***3.4 Interpolating monthly NDVI images***

Given that many methods have been devoted to reorganizing the trajectory of a time series, a viable approach to emulate satellite data NDVI time-series should be proposed to ensure integrity before seasonal analysis (Tang et al., 2010). The method for generating a monthly time series is usually summarized as feature fitting. Conversely, the results of some curve fitting methods are very strictly then the effectiveness of real detection can be reduced to effectiveness of detecting

phenomenon of agriculture (Xiang et al., 2007, Yan et al., 2016). The linear interpolation algorithm between the two images can be described as follows:

$$\frac{NDVI - NDVI_0}{DOY - DOY_0} = \frac{NDVI_1 - NDVI_0}{DOY_1 - DOY_0}$$

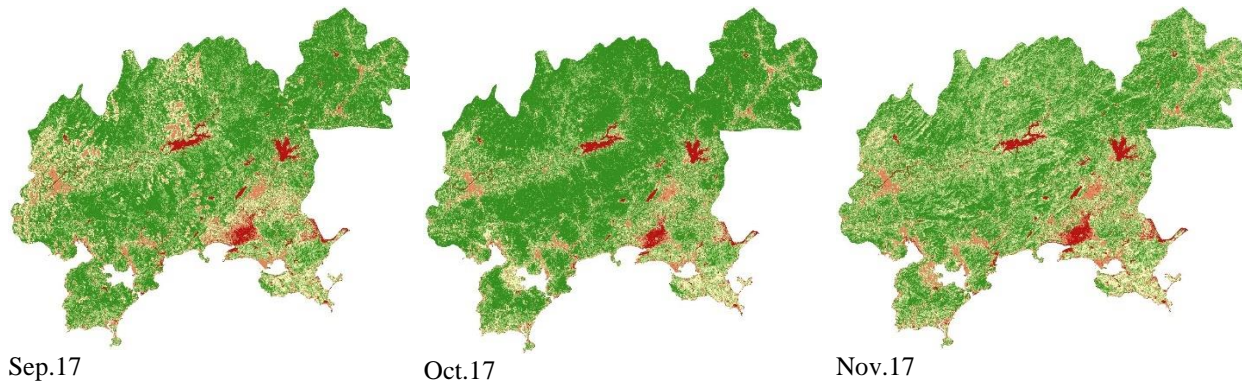
Where, NDVI represents the missing day to be interposed.  $NDVI_1$ ,  $NDVI_0$  represents the valid observations used for the interpolation. Therefore, NDVI is considered as a liner relation between  $NDVI_0$  and  $NDVI_1$ :

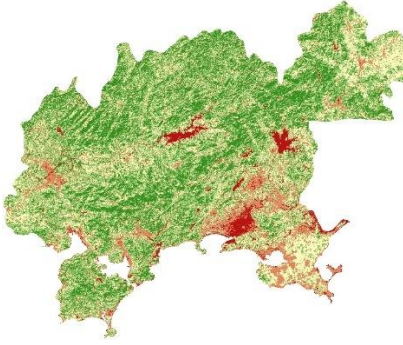
$$NDVI = NDVI_0 + (NDVI_1 - NDVI_0) * \frac{DOY - DOY_0}{DOY_1 - DOY_0}$$

Therefore, every NDVI for such a particular day can be obtained among two good observations. Apparently, the frequency of NDVI images determines how well the liner interpolation performs. We used ArcGIS software to achieve an image based monthly NDVI time series.

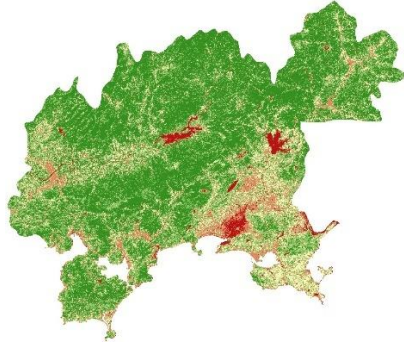
#### 4. Results & Discussion

NDVI time series has been used to examine the relation between spectral variability and changes in the agriculture growth rate or phenology change. It is also useful to determine the changes in agriculture production. The results, which are indicated in Figure 2, represent different months NDVI time series of the study area.

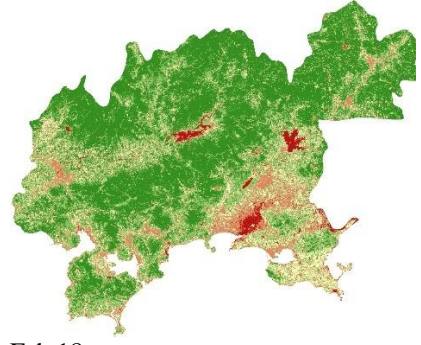




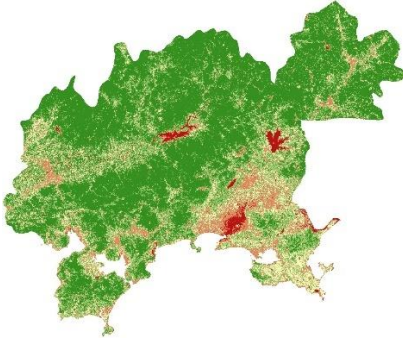
Dec.17



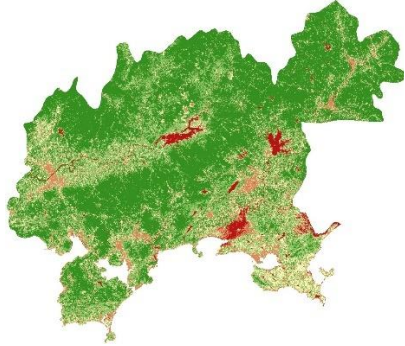
Jan.18



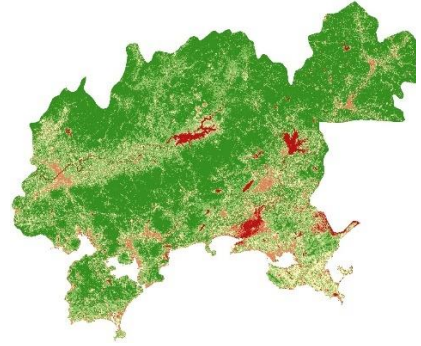
Feb.18



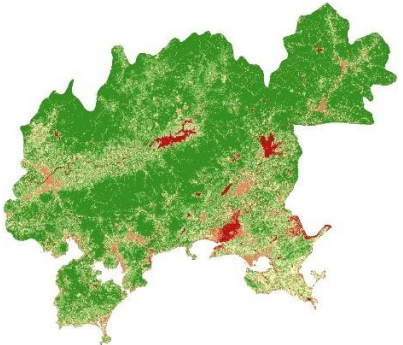
Mar.18



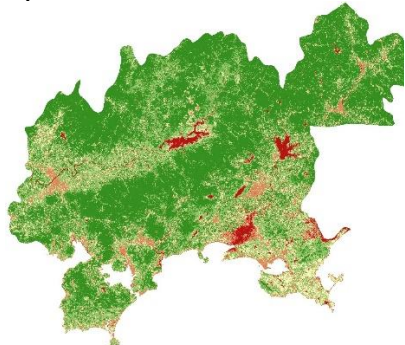
Apr.18



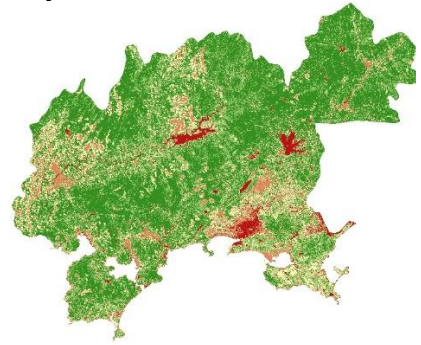
May.18



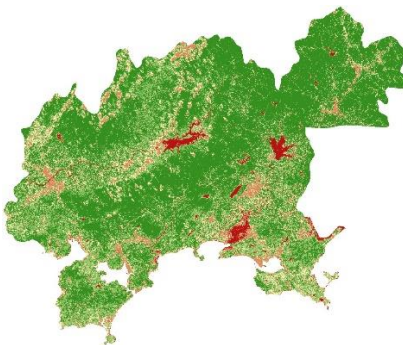
Jun.18



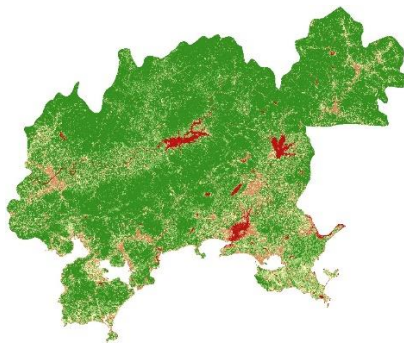
Jul.18



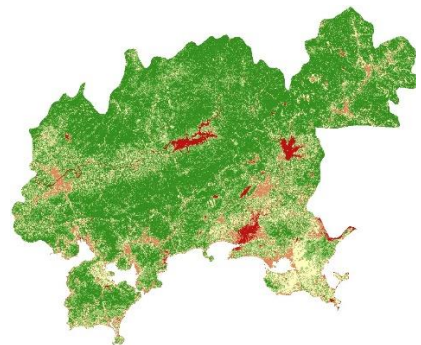
Aug.18



Sep.18



Oct.18



Nov.18



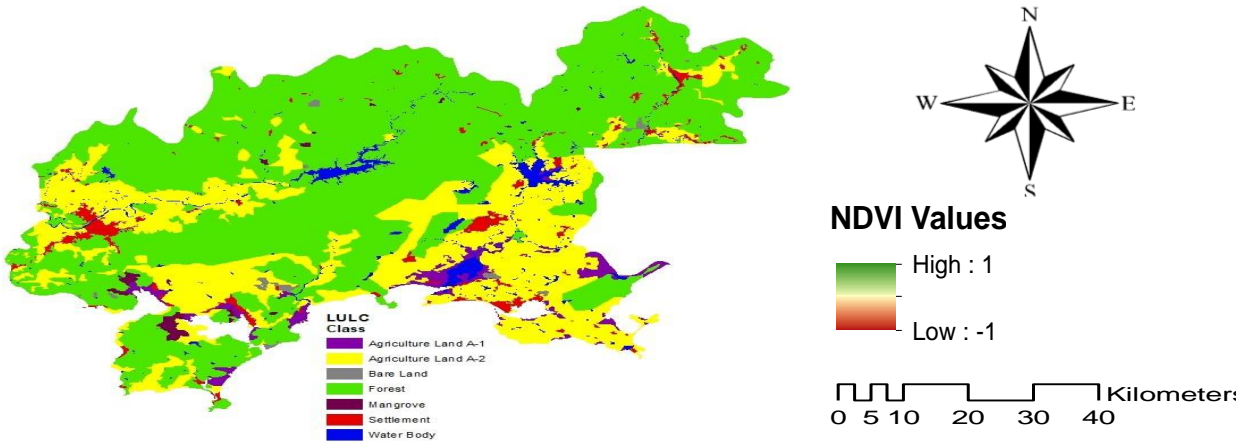
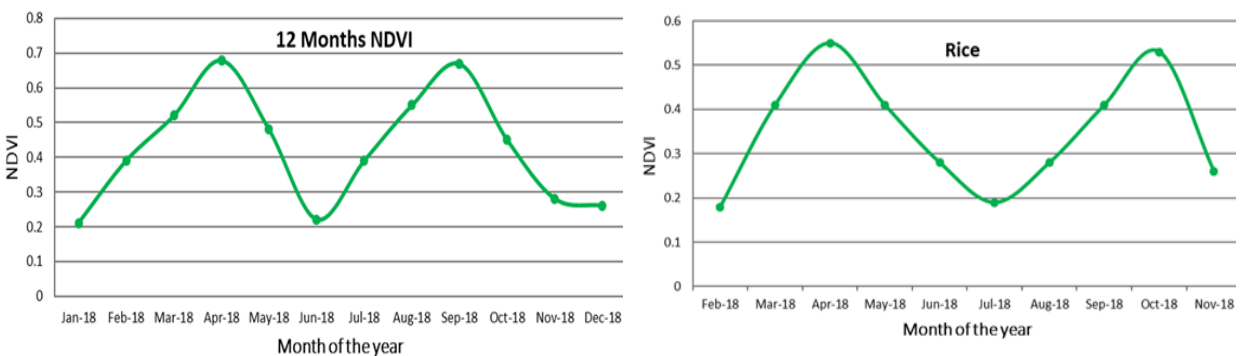


Fig. 2. Remote sensing satellites based NDVI time series maps.

We initially accomplish LULC classification and determine the relevant land cover categories in the study region: farmland, bare land, forest, mangrove, water, and built-up land before analyzing all images (Fig. 2). It was important to know the exact area and location of the agriculture fields in the study area. We found that multispectral images are giving the best results for all the characteristics of the NDVI values with the changes of the every month. In this work, NDVI values were same as shown in figure 2 and 3. The lowest values were found on low vegetation and highest values for crop flowering time. From no vegetation class maximum reflection was from the soil so the NDVI values was low and from crop land NIR and Red bands produces high reflection so produce high NDVI values. The NDVI time series demonstrated a phenology high associated with crop growth. As its high value indicated in April and September months and low value indicated in June month (Fig. 3). The NDVI time series from January to December shows the differences of the entire year in figure 3.



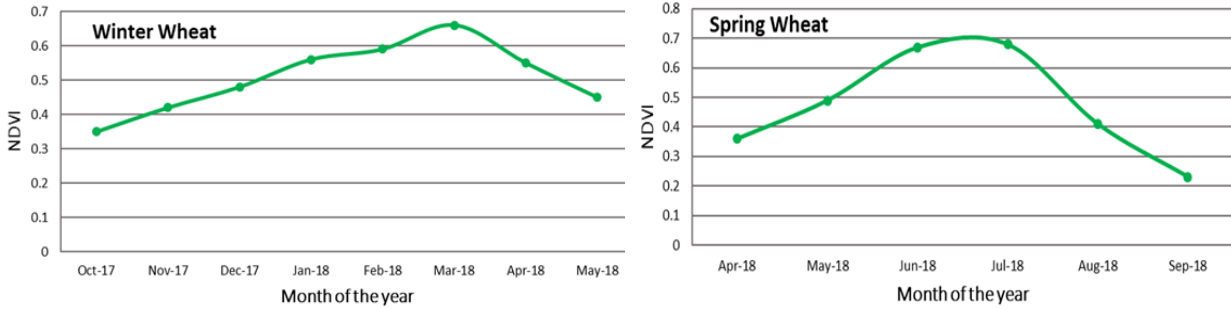


Fig. 3. Mapping crop phenology using NDVI time series from 2017 – 2018.

To categorize the crop varieties, all the data were verified to the crop calendar. The type of crop in this study area is seasonal; hence the value of NDVI varies from time to time. The NDVI graph demonstrates the low values indicated from the months of June and July as well as high in April and September. Results indicated the winter wheat crop date of season start/end (October/May) planting and harvest, date of spring wheat season start/end (April/September). In the month of March and April, the winter wheat crop reaches its peak. Rice planting time is February/July and harvesting time is Jun/November. The highest values of NDVI were collected in the month of April and October. Rice is partially covered with water in June, so reducing NDVI values and reaching the peak NDVI values at the beginning of August / September. In summary crop phenology graph associated with crop calendar. NDVI measurements were used to compute total agricultural data. To begin, we define NDVI values according to table 1.

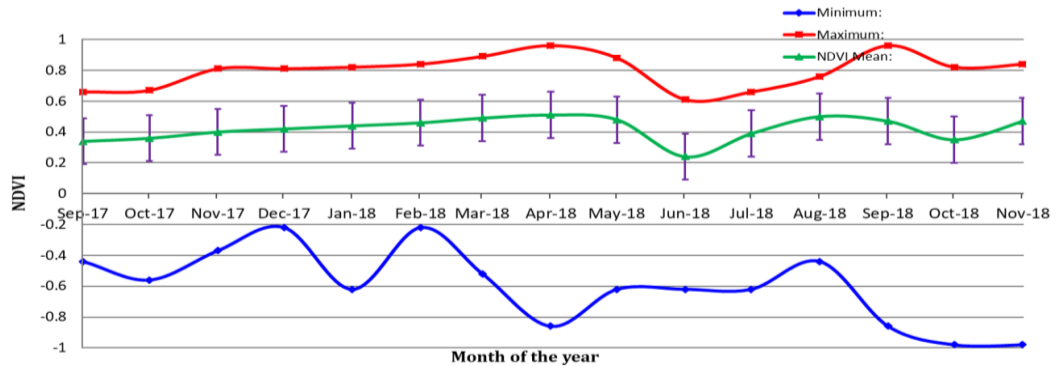
Table 1 NDVI Classification

NDVI Class	Agriculture condition/health
> 0.7	Very high agriculture
0.6 – 0.7	High agriculture
0.4 – 0.6	Medium agriculture
0 – 0.4	Low agriculture
< 0	No agriculture

We choice four city, so first we split whole vegetation section according to NDVI classification (table 1). After that we separated the agriculture land and divided according to NDVI classes. The highest NDVI value (0.51 NDVI) was recorded in April/September, while the lowest was recorded

in June (0.24 NDVI). In the summer, the maximum NDVI values in the study area approach 0.96, indicating very robust agriculture due to favorable meteorological conditions (fig. 4). Therefore, this area has high production rates. NDVI values grow faster from November (from sowing and emergence) to February. It reached its highest growth in March. Also, it's remained relatively stable in April and May. It recorded its highest growth rate in March and remained stable in April and May.

NDVI minimum, maximum and mean Agriculture



NDVI minimum, maximum and mean Vegetation

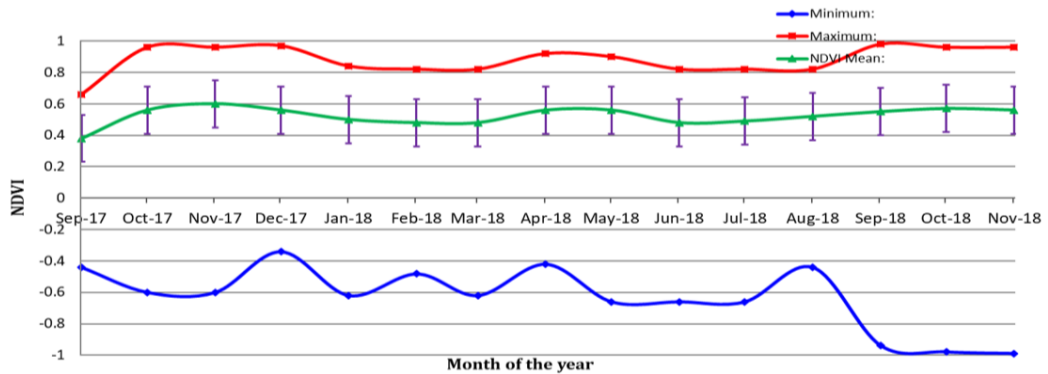


Fig. 4 Crop phenology graph in the study area with minimum, maximum and NDVI mean.

After that, NDVI gradually declined and its matured time in May and harvesting time in June. In vegetation low NDVI months are January, June, July and high NDVI months are November, December, April (table 2).

Table 2 Agriculture and vegetation NDVI changes from Sep.2017 to Nov.2018.

	Vegetation			Agriculture		
NDVI	Minimum	Maximum	NDVI mean	Minimum	Maximum	NDVI mean

Sep.17	-0.44	0.66	0.38	-0.44	0.66	0.34
Oct.17	-0.6	0.96	0.56	-0.56	0.67	0.36
Nov.17	-0.98	0.96	0.61	-0.37	0.81	0.4
Dec.17	-0.34	0.97	0.56	-0.22	0.81	0.42
Jan.18	-0.62	0.84	0.51	-0.62	0.82	0.44
Feb.18	-0.48	0.82	0.48	-0.22	0.84	0.46
Mar.18	-0.62	0.82	0.48	-0.52	0.89	0.49
Apr.18	-0.42	1	0.56	-0.86	0.96	0.51
May.18	-0.66	1	0.56	-0.62	0.88	0.48
Jun.18	-0.67	0.82	0.48	-0.23	0.56	0.24
Jul.18	-0.66	0.82	0.49	-0.42	0.69	0.39
Aug.18	-0.44	0.88	0.52	-0.44	0.76	0.5
Sep.18	-0.94	1	0.55	-0.86	0.96	0.47
Oct.18	-0.98	0.98	0.57	-0.98	0.82	0.35
Nov.18	-1	0.97	0.56	-0.98	0.84	0.47

As NDVI time series crop phenology was show that total vegetation area is 6601.16 km<sup>2</sup> and agriculture area is 2010.46 km<sup>2</sup>. Hence, during this period the maximum agriculture sector comes from the medium NDVI sector (fig 6). From October to May we find all NDVI values classes (table 3) in agriculture area and in vegetation area month are September to May which is show that in 2018 vegetation was increase (fig. 5).

Table.3 Agriculture and vegetation area (km<sup>2</sup>) change metrics from Sep.2017 to Nov.2018.

NDVI Class	Very high	High	Medium	Low	No	Very high	High	Medium	Low	No
NDVI Value	>0.7	0.6-0.7	0.4-0.6	0-0.4	<0	>0.7	0.6-0.7	0.4-0.6	0-0.4	<0
	<b>Vegetation</b>					<b>Agriculture</b>				
Sep.17		30.96	4628.09	2355.62	186.48		202.72	1013.44	702.29	86.01

Oct.17	190.16	1058.09	3790.08	2611.28	141.55		459.74	929.96	582.98	37.78
Nov.17	241.01	1080.1	2600.08	2900.02	173.46		520.21	402.61	1000.13	87.72
Dec.17	260.01	1070.2	2206.57	2803.08	159.5	110.1	796.2	130.71	900.8	72.75
Jan.18	1790.59	1881.08	1706.66	1035.38	187.45	167.01	402.13	680.31	693.9	67.11
Feb.18	1003.02	2012.02	2369.94	1056.87	159.31	110.2	599.05	133.49	1185.15	82.57
Mar.18	1489.48	2665.55	1082.49	1233.77	129.87	111.06	361.65	832.54	664.76	40.45
Apr.18	2462.48	1399.22	1731.25	900.97	107.26	207.2	240.35	901.73	624.18	37.01
May.18	1672.44	2860.12	1224.46	658.06	186.08	120.76	640.67	826.13	363.42	59.48
Jun.18		2860.06	1423.46	2131.56	186.09		421.15	746.13	884.18	59.48
Jul.18		1931.33	3799.17	685.82	184.84		644.65	938.58	366.48	60.75
Aug.18		327.76	4031.14	2055.62	186.64		215.31	1000.85	702.29	92.01
Sep.18	441.45	2043.08	2181.16	1748.32	176.15		306.29	910.68	738.89	53.63
Oct.18	1099.55	1728.78	2944.68	648.27	179.88	142.92	565.2	910.25	336.33	55.76
Nov.18	1397.8	2640.08	1595.26	795.63	172.88	155.28	593.41	761.45	449.85	44.47

Winter wheat planting time is September and harvesting time is end of May. During this period we find very high NDVI classes in the December to April with 1,124.53 km<sup>2</sup> area.

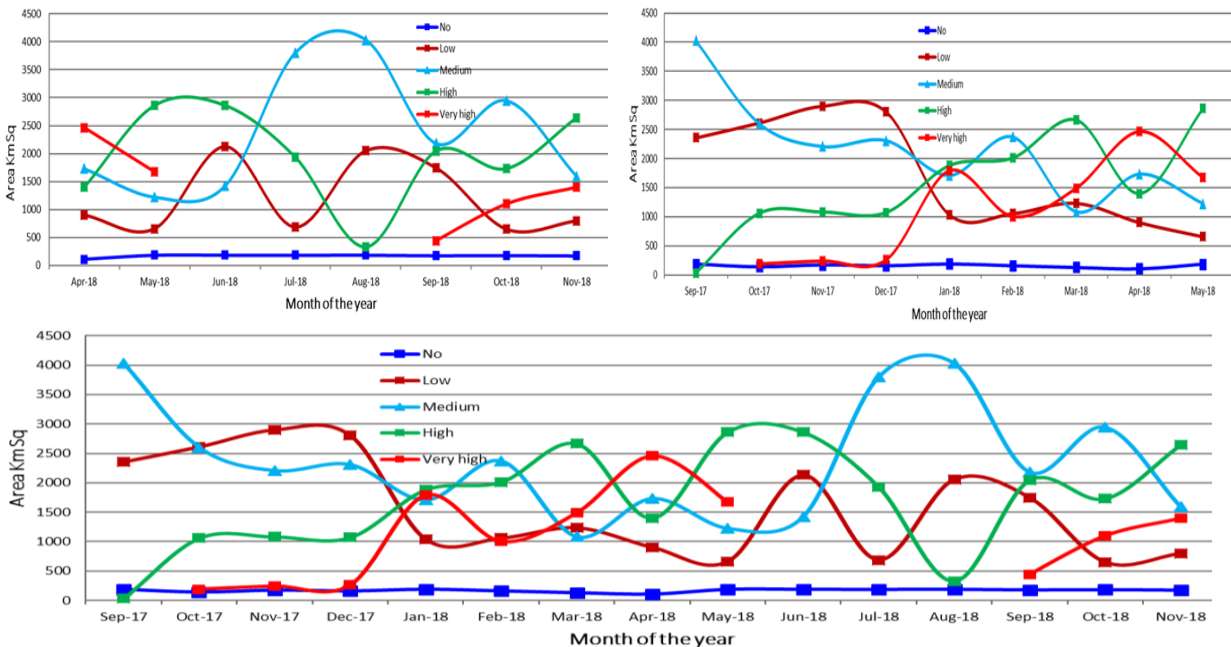


Fig. 5. Vegetation NDVI area graph.

Summer wheat planting time is April/ May months and harvesting time is October / November. In this time sun light is too much that`s why all crop is growing too fast to maturity. Very high area covered by medium NDVI sector. North study areas most cropping is wheat and rice but near the sea area rice is a major crop that`s why here NDVI values are low.

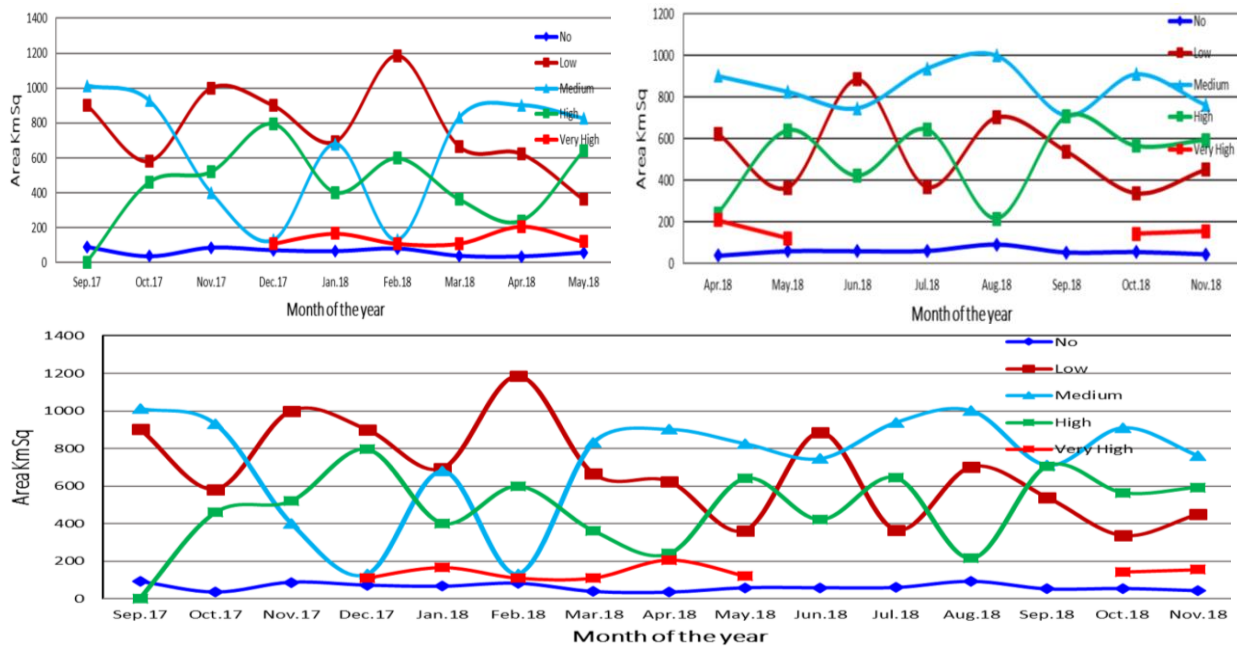


Fig. 6. Winter wheat & Spring wheat NDVI area graph (Agriculture)

We can immediately detect NDVI standard statistical variations inside the monthly NDVI graphs (fig. 7). We use Google Earth for accuracy evaluation because it has very high-resolution imagery. For example, the maximum likelihood supervised classification method was used to successfully identify the planting areas of wheat and rice crop areas. Remote sensing will help in identifying yield monitoring the related agriculture areas. Estimation of crop yield by using the vegetation index can achieve the overall accuracy of approximately 92%.



Fig. 7. Field photographs. (Sources: Google)

## 5. Conclusion

In this study, we propose an elaborate analysis technique for create of NDVI time-series with the smoothing technique of the filter being aimed to minimize the error component from the original equation. Without involving multi-temporal remote sensing data of different sensor, the information content on the major agricultural crops could not be obtained. With multispectral data, many crops differ from one to another in a certain stage in the growing phase. The Sentinel data have great feasible in agriculture monitoring, especially mapping of crop planting areas, monitoring of crop growth, and estimating crop yield (Wang et al., 2019).

We described the technique of NDVI time analysis in phenology categorization. The NDVI method gives better results were obtained using the spectral band defined by crop multipurpose NDVI profile and additional multi-temporal. The calculated agriculture requirements were consistent with available reference information. Depending on the time of crops, other temporal features could be determined of classification.

Furthermore, a technique for recreating time-series was established, while it will be improved in the mapping of plant phenology by the previous researcher. The planting and harvesting dates can be beneficial for water management, fertilization, nutrition, and cultivation assessments. Future work will consider additional usage of radar data, for which some initial tests were very promising because they show an overall accuracy increase.

## Acknowledgments

This work is done through a PhD scholarship from PolyU Hong Kong and research grants from the Research Grants Council (HKSAR) grant project codes B-Q49D and 1-ZVE8. Authors would also like to acknowledge the support drawn from the Lands department and Agriculture department of Guangdong, China.

## References

1. Ahmadi H, Nusrath A. 2012, "Vegetation change Detection of Neka river in Iran by using remote sensing and GIS", *Journal of geography and Geology*, 2 (1)., pp. 58-67.
2. Alex O. O., George A. B., Jingfeng H., Wenjiang H. 2018, Applications of satellite 'hyper-sensing' in Chinese agriculture: Challenges and opportunities. *International Journal of Applied Earth Observation and Geoinformation*. Vol 64, pp 62-86.
3. Atzberger C. 2013. Advances in remote sensing of agriculture, Context description, existing operational monitoring systems and major information needs. *Remote Sensing*, 5, 949– 981.
4. Aadhar, S., Mishra, V., 2017. High-resolution near real-time drought monitoring in South Asia. *Sci. Data* 4, 170145. <http://dx.doi.org/10.1038/sdata.2017.145>.
5. Chen, J., Huang, J., Hu, J., 2011. Mapping rice planting areas in southern China using the China Environment Satellite data. *Math. Comput. Modell.* 54, 1037–1043.
6. Esch, T., Metz, A., Marconcini, M., Keil, M., 2014. Combined use of multi-seasonal high and medium resolution satellite imagery for parcel-related mapping of cropland and grassland. *Int. J. Appl. Earth Obs. Geoinf.* 28, 230–237.
7. Estel, S., Kuemmerle, T., Levers, C., Baumann, M., Hostert, P., 2016. Mapping cropland-use intensity across Europe using MODIS NDVI time series. *Environ. Res. Lett.* 11 024015–024015.
8. Fan, M.S., Shen, J.B., Yuan, L.X., Jiang, R.F., Chen, X.P., Davies, W.J., Zhang, F.S., 2012. Improving crop productivity and resource use efficiency to ensure food security and environmental quality in China. *J. Exp. Bot.* 63, 13–24.
9. Gnyp, M.L.; Miao, Y.X.; Yuan, F.; Ustin, S.L.; Yu, K.; Yao, Y.K.; Huang, S.Y.; Bareth, G. 2014. Hyperspectral canopy sensing of paddy rice aboveground biomass at different growth stages. *Field Crop. Res.*, 155, 42–55.



10. Gommers, R., Wu, B., Zhang, N., Feng, X., Zeng, H., Li, Z., Chen, B., 2017. Crop Watch agroclimatic indicators (CWAIs) for weather impact assessment on global agriculture. *Int. J. Biometeorol.* 61, 199–215.
11. Hansen M C, Loveland T. 2012. A review of large area monitoring of land cover change using Landsat data. *Remote Sensing of Environment*, 122, 66–74.
12. Harmon, T., Kvien, C., Mulla, D., Hoggenboom, G., Judy, J., Hook, J., 2005. Precision agriculture scenario. In: Arzberger, P. (Ed.), *NSF Workshop on Sensors for Environmental Observatories*. World Tech. Evaluation Center, Baltimore, MD, USA.
13. He, C., Liu, Z., Xu, M., Ma, Q., Dou, Y., 2017. Urban expansion brought stress to food security in China: evidence from decreased cropland net primary productivity. *Sci. Total Environ.* 576, 660–670.
14. Liang, L.; Di, L.P.; Zhang, L.P.; Deng, M.X.; Qin, Z.H.; Zhao, S.H.; Lin, H., 2015. Estimation of crop LAI using hyperspectral vegetation indices and a hybrid inversion method. *Remote Sens. Environ.* 165, 123–134.
15. Meng, J.H., Wu, B.F., Li, Q.Z., Du, X., 2009. Monitoring crop phenology with MERIS data – A case study of winter wheat in North China Plain. In: *Progress in Electromagnetics Research Symposium*. Beijing, China.
16. Sakamoto, T., Yokozawa, M., Toritani, H., Shibayama, M., Ishitsuka, N., Ohno, H., 2005. A crop phenology detection method using time-series MODIS data. *Remote Sens. Environ.* 96, 366–374.
17. Shi Y, Ji S, Shao X, Tang H, Wu W, Yang P, Zhang Y, Shibasaki R. 2014. Framework of SAGI agriculture remote sensing and its perspectives in supporting national food security. *Journal of Integrative Agriculture*, 13, 1443–1450.
18. Tang H, Wu W, Yang P, Zhou Q, Chen Z. 2010. Recent progresses in monitoring crop spatial patterns by using remote sensing technologies. *Scientia Agricultura Sinica*, 43, 2879–2888.
19. Xiang, L.I., Yu-chun, P.A.N., Zhong-qiang, G.E., Chun-jiang, Z., 2007. Delineation and scale effect of precision agriculture management zones using yield monitor data over four years. *Agric. Sci. China* 6, 180–188.

20. Yan, L., Roy, D.P., Zhang, H.K., Li, J., Huang, H., 2016. An automated approach for subpixel registration of Landsat-8 Operational Land Imager (OLI) and Sentinel-2 Multi Spectral Instrument (MSI) imagery. *Remote Sens.* 8 (6), 520.
21. Wang Y., Xue Z., Chen J., 2019. "Spatio-temporal analysis of phenology in Yangtze River Delta based on MODIS NDVI time series from 2001 to 2015." *Front. Earth Sci.* Vol.13 (1) pp. 92-110. <https://doi.org/10.1007/s11707-018-0713-0>.